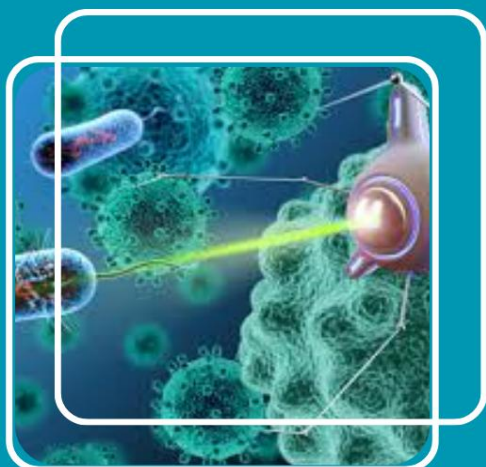


MJ MULTISCIA
JOURNALS PUBLISHERS

FRONTIERS IN MATERIAL SCIENCE AND NANOTECHNOLOGY

ISSN: (3065- 4114)



✉ editor.fmsnt@gmail.com

<https://multisciajournals.com/journals/index.php/fmsnt>



Achieving Atomically Flat Mica Surfaces via the Growth of Gold Nanoprisms

Marchenko OS

Department of Material Science and Nanotechnology

Article Info

Received: 29-04-2025 Revised: 02-06-2025 Accepted: 11-06-2025 Published: 22-06-2025

Abstract

Synthesis of gold nanoparticles (NPs) in liquids, micelles, and at various interfaces is being done using a variety of approaches. Parameters of synthesis determine the size and shape of NPs. Our proposal here is to generate Au NPs on mica surfaces that are atomically flat. Under these circumstances, the surface is undergoing the simultaneous formation of monocrystalline and isotropic NPs. Monocrystalline prism-like nanoparticles (NPRs) are being preferentially formed at the synthesis parameters that we have identified. A surface's wettability is one factor that determines the proportion of NPRs with a triangular or hexagonal habit. We show that growth medium components and synthesis settings may regulate the size and shape of produced NPs.

Keywords: Nanoparticles; Nanoprisms; Surface wetting angle; Polyvinylpyrrolidone; Ethanol; Ethylene glycol; Glycerol

Introduction

There has been a lot of interest in studying gold nanoparticles (NPs) in recent decades. Gold nanoparticles (Au NPs) have many applications in fields as diverse as medicine [1-6], optoelectronics [7-13], catalysis [14-16], and surface plasmon resonance (STM) and scanning tunneling resonance (SERS) [17–20]. Synthesis of gold nanoparticles in micelles and at phase interfaces has been the primary focus of most research. A lot less focus has been spent creating regular-shaped monocrystalline NPs (sometimes termed "nanoprisms" or NPRs) on solid surfaces. The authors of the study described the formation of gold nanowires and nanoplates on indium tin oxide-coated glass surfaces by the use of cetyltrimethylammonium bromide in aqueous medium [18]. Using a one-step thermolysis of a (AuCl₄)- tetraoctylammonium bromide complex in air, gold NPRs have been produced on solid substrates (Si, glass, stainless steel, polyimide, polydimethylsiloxane (PDMS), mica, graphite, etc.) in references [21, 22]. Au NPRs may be synthesized using either one- or multi-stage techniques. Proposed in [23-25] and revised in [26-27] was the nucleus approach of NPRs creation. Hence, the whole process may be summarized as follows: nuclei production, growth media condition changes, nuclei addition to growth medium, and finally, NPR development. The problem is that this kind of synthesis produces nanostructures that aren't uniformly spherical and anisotropic; so, further purification is required. Biosynthesis, photoreduction, the thermal technique, and polyol synthesis are all examples of one-stage processes. In biosynthesis, products of essential microbial processes [28–29], plant extracts [30], and fungi [31] are used as Au ion reducers and NPR stabilizers. In order to conduct photoreduction, a growth medium must have a photocatalyst, a stabilizer, and an electron-donating chemical [32]. Through adjusting (i) the ratio of precursor/stabilizer concentration, (ii) the synthesis time, and (iii) the temperature, thermal and polyol techniques enable the control of NPRs in a broad range of sizes [33]. Unless polyol (120-195° C), none of the aforementioned procedures need high temperatures. The EG acts as a dispersion medium and Au ion reducer in this process, while the PVP or PVP+CTAB combination [34–38] serves as a stabilizer. Flat, hexagonal or triangular Au nanocrystals with a thickness of less than 100 nm were created in a free volume of a combination of ethanol, ethylene glycol, HAuCl₄ (a gold precursor), and PVP at 80° C using the polyol technique, as described in reference [38]. By including glycerol, we suggest a modified polyol approach. Our findings show that the development characteristics are significantly altered when newly sliced mica plates are immersed in the growth media. This environment is ideal for the simultaneous formation of gold NPRs and NPs on mica surfaces. Increasing the synthesis time or adding glycerin to the mixture both cause to NPRs are formed preferentially. Through surface wetting angle (SWA) measurements, the impact of growth medium components on the creation of gold nanostructures on atomically flat mica substrate that had just been cut was investigated. The goal of this research is to examine how Au nanostructures form on mica surfaces that are atomically flat when submerged in growth media of varying compositions.

Materials and Methods

The following ingredients were used to create gold NPRs on the newly cleft surface of mica: ethyl alcohol, polyvinyl pyrrolidone (29 kDa, "Sigma-Aldrich"), ethylene glycol ("Reahim ", Russia), glycerin ("Sigma-Aldrich"), and chloroauric acid ("Shanghai Synnad Fine Chemical Co., LTD"). A scanning electron microscope (SEM) (X-ray microanalyzer JXA-733 with energy dispersive X-ray spectrometer) and a scanning electron microscope (JSM-6060) were used to study the chemical content and shape of the gold nanostructures that were formed. The following parameters and analytical features were used to estimate the chemical composition using EDS: an accelerating voltage of 20 kV, a beam current of 20 nA, a spectral resolution of 140 eV at line MnK α , and a spatial resolution of 1–5 microns. The reference materials were Si, Al, Mg, FeO (SiO₂, Al₂O₃, MgO, FeO, biotite), Mn (metal Mn), Ti

(ilmenite), and Au (Au). The recalculations technique was ZAF (atomic number of the Z, A absorption, fluorescence F), and the detection limit was 0.01-0.1%. Through surface wetting angle (SWA) measurements, the impact of growth medium components on the creation of gold nanostructures on atomically flat mica substrate that had just been cut was investigated. A newly sliced surface of bare mica and an annealed surface of Au (111) were each treated with a droplet of the respective component. The amount of droplets that were deposited was 2 microliters. After taking five separate readings, we were able to average the contact angle value. Within $\pm 5^\circ$ was the margin of error for the measured wetting angle.

Results

Synthesis I

15 ml of ethylene glycol (EG) was mixed with 1.6 ml of ethanol (ET). Than 2ml of PVP C=0,45M (molar concentration per polymer repeating unit) and 1.4 ml of H_{Au}Cl₄ solution (C_{Au}=1600 mg/dm³) were added. A freshly cleaved mica plates (10 mm×6mm) were placed vertically in the glass tubes with 5ml of growth medium. Formation of gold nanostructures was held during 24 hours at 80 ° C. The obtained crystals have triangular and hexagonal shape with the lateral dimensions from 30nm up to 20 microns depending on the ratio concentrations of H_{Au}Cl₄, PVP and the time of synthesis. Such conditions contribute to reduction of Au ions via ET, while EG led to reduction at higher temperatures - 120÷165 ° C [39,40]. The time of synthesis was varied up to 24 hours.

Immersing of mica plate into the growth medium changed the conditions of nucleation. Nucleation occurs in free volume (homogeneous nucleation) as well as on the surface of mica (heterogeneous nucleation). Percentage of NPRs depends on surface conditions, in particular, wettability determined by growth medium. The results of SWA measurements are presented in Table 1.

| Component | | Surface wetting angle θ , ° | |
|-----------|---|------------------------------------|------|
| | | Au(111) | Mica |
| 1 | EG | 38 | 30 |
| 2 | ET | <9 | <9 |
| 3 | ET:EG(1:3) | <9 | 19 |
| 4 | ET:EG(1:3), PVP | <9 | 41 |
| 5 | ET:EG(1:3), PVP. H _{Au} Cl ₄ | <9 | 17 |

Table 1: Surface wetting angle according to the composition of the growth medium ET: EG (1:3)

The contact angle of EG with mica surface is $\theta=30^\circ$, while ET droplet completely spreads on the surface. Adding PVP up to 0,045M concentration in the mixture ET+EG changes the contact angle more than 2 times-up to 41° (against 19° without PVP, see Table 1). It can be due to adsorption of PVP on mica surface. PVP molecules attach to the substrate via pyrrolidone (γ -Lactam) ring of linear polymer units while - OH groups are located in the opposite direction.

Adding of H_{Au}Cl₄ in growth medium (0.5 mM) does not change the wetting of Au (111) surface while the wetting angle for bare mica drops down up to 17° . Thus, the surface of the gold film is completely wetted by growth medium (row 2-5 for Au (111) in table 1), *ie.*, attraction between Au atoms and components of growth medium is sufficiently strong.

Exposition of mica plate into growth medium (see row 5, Table 1) leads to the formation of gold nanostructures on the surface during 24 hours. As can be seen in SEM images (Figure 1) the surface of a freshly cleaved mica is preferentially covered by aggregates of Au NPs. The shape of the most nanoparticles is nearly spherical. The particles are covered by thin film of PVP stabilizer (gray «aura» around NPs, Figure 1b-d). The adsorbed film prevents coalescence of NPs. However, the particles are self-assembled into separate areas. Aggregate of NPs is depicted in Figure 1d with tilt of substrate to the direction of electron beam at 60° . Flat NPRs with triangular and hexagonal habit rarely appear as well as nanowires (Figure 1c, right nner).

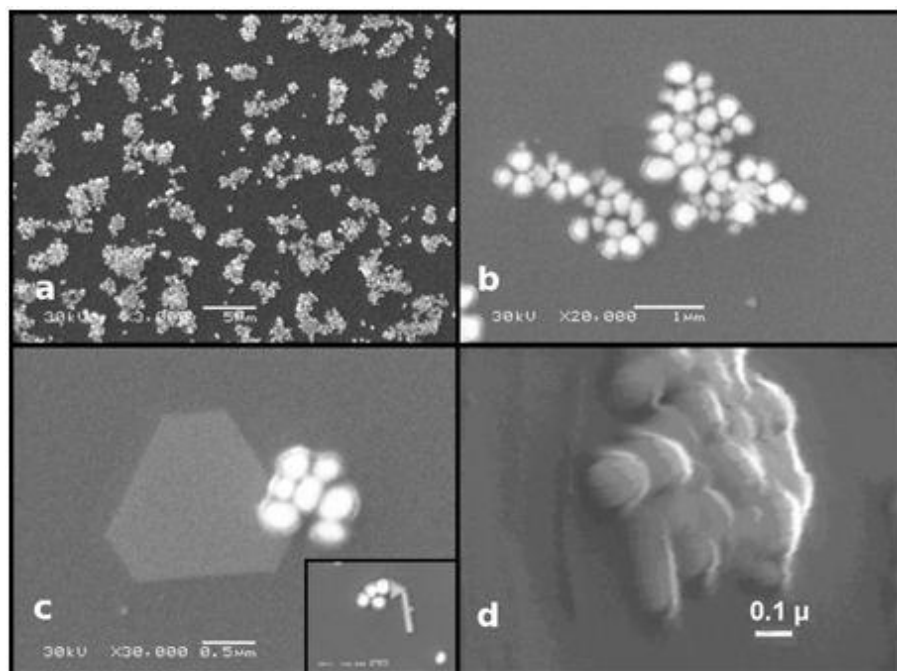


Figure 1: SEM images of gold nanoparticles on mica surface. The growth medium - ET:EG (1:3); 0.5 mM HAuCl₄; 0,045M PVP; time of synthesis t=24 hours

Synthesis II

In order to increase the number of gold NPRs per unit area the conditions of synthesis were changed: (i) in growth media glycerol G is added, (ii) concentration of gold and synthesis time (t=48 h) is increased. The growth medium contained ET:EG:G (6:7:7), HAuCl₄ (1 mM) and PVP (0,045M). Adding of G increases viscosity of dispersion medium. Table 2 demonstrates the dynamic viscosity. The value of η_G is an order of magnitude greater than η_{EG} and exceeds η_{ET} more than 70 times Table 2.

| Alcohol | Dynamic viscosity η , 10-3Pa.s | Alcohol |
|---------|-------------------------------------|-------------|
| ET | 1,2 (20° C) | 0,5 (70° C) |
| EG | 19,9 (20° C) | 3,2 (80° C) |
| G | 1480 (20° C) | 35 (80° C) |

Table 2: Temperature dependence of surface tension and dynamic coefficient of viscosity of alcohols

However, adding of G enhances wettability of mica surface. Table 3 shows the results of SWA measurements for mica surfaces and annealed Au (111).

| Component | Surface wetting angle θ , ° | |
|---|------------------------------------|------|
| | Au(111) | Mica |
| 1 G | 37 | 21 |
| 2 EG | 38 | 30 |
| 3 ET:EG:G (6:7:7) | <9 | <9 |
| 4 ET:EG:G (6:7:7); 0,045M PVP | <9 | <9 |
| 5 ET:EG:G (6:7:7); 0,045M PVP; 1mM HAuCl ₄ | <9 | <9 |

Table 3: Dependence of wetting angle on composition of the growth medium G:EG:ET (7:7:6)

In contrast to the system of ET:EG(1:3), adding of PVP into a dispersion medium ET:EG:G (6:7:7) increases lyophilicity of mica surface.

Thus, the redox atoms in growth medium (see Table 3, row 5) are attached much stronger to the mica surface, and the quantity of NPRs is increased. This hypothesis was experimentally confirmed.

To remove deposited NPs which attached to surface from free volume samples were rinsed in distilled water (Figure 2). Thereafter, we found that NPRs were randomly distributed on the substrate. The most of nanostructures demonstrate regular triangle and hexagonal shape or triangles with truncated vertices.

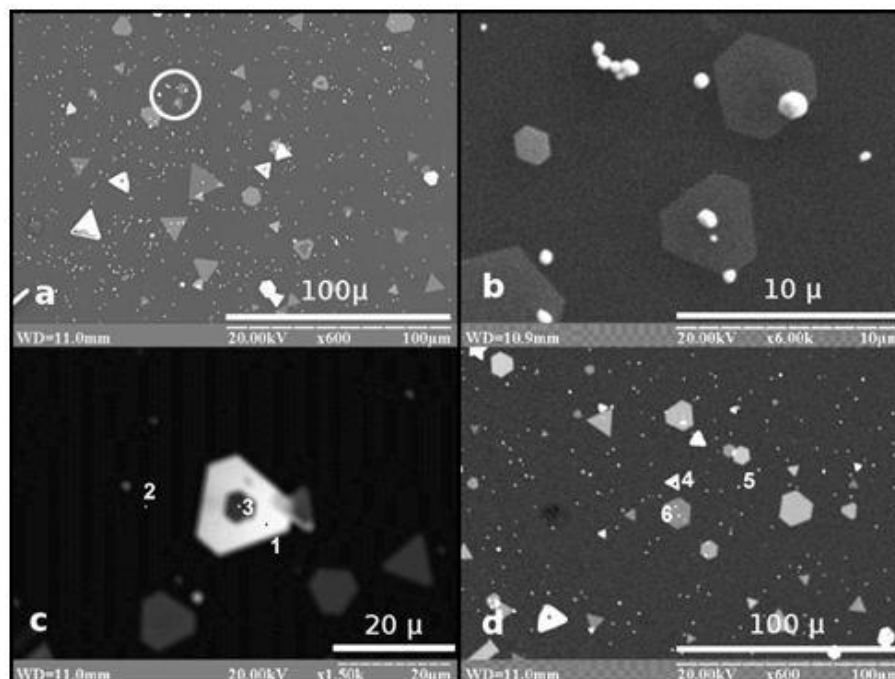


Figure 2: SEM images of gold NPs and NPRs on the surface of mica after rinsing in distilled water. The growth medium: ET: EG: GL (6:7:7); 1 mM HAuCl₄; 0,045M PVP; synthesis time t=48 hours. Numbers denote the points at which the energy dispersive spectra were taken: 1 and 4 - the surface of the thick NPRs, 2 and 5 - mica substrate, 3 - the cavity inside NPRs, 6 - a thin gold NPRs. *b is an enlarged circular region of image a.

The element composition of the substrate and NPRs was investigated (Table 4). Semi-quantitative microprobe analysis was carried out by EDS. The results in Table 4 are normalized. Analysis shows that the mica substrate is muscovite which includes ~ 46% SiO₂, ~ 34% Al₂O₃ and minor impurities of Na₂O, MgO, K₂O, TiO₂ and FeO (Table 4, columns 2 and 5).

| Elemental composition (%) | Point number | | | | | |
|--------------------------------|--------------|-------|-------|-------|-------|-------|
| | 1 | 2 | 3 | 4 | 5 | 6 |
| SiO ₂ | 0,00 | 47,10 | 38,28 | 9,98 | 45,93 | 39,12 |
| TiO ₂ | 0,00 | 0,30 | 0,46 | 0,05 | 0,40 | 0,43 |
| Al ₂ O ₃ | 0,00 | 33,30 | 27,46 | 8,23 | 35,88 | 29,02 |
| FeO | 0,00 | 1,70 | 2,28 | 2,50 | 1,61 | 2,42 |
| MnO | 0,00 | 0,00 | 0,03 | 0,30 | 0,00 | 0,17 |
| MgO | 0,00 | 2,30 | 1,82 | 0,75 | 2,21 | 1,85 |
| Na ₂ O | 0,00 | 1,50 | 0,00 | 0,00 | 1,51 | 1,14 |
| K ₂ O | 0,00 | 13,80 | 16,75 | 13,22 | 12,56 | 15,93 |
| Au | 100 | - | 12,92 | 64,97 | - | 9,92 |
| Sum | 100 | 100 | 100 | 100 | 100 | 100 |

Table 4: Semi-quantitative microprobe analysis of individual points of the mica surface

Energy dispersive spectrum at point 1 indicates 100% of gold (Table 4, column 1) *i.e.* investigated nanoprism is formed by gold. The thickness is large enough to prevent penetration of electron beam. Thus, there are no other lines in the spectrum except of intensive L α (9,7 keV), L β 1 (11,45 keV) and weaker lines of gold M α (2,12 keV) and M β (2.2 keV) (see support materials).

Discussion

It is possible to use the LaMayer model to analyze the mechanism of development of Au NPs and NPRs during polyol synthesis processes [41]. In the first step, AuCl₄-ions undergo reduction to Au⁰. Afterwards, nuclei are created in the locations with the highest concentration of Au⁰. When their size is below critical, nuclei may decay; when they're larger than critical, they can increase. In the last step, the growth rate and diffusion of atoms on the surface of the NPs restrict the augmentation in size of the NPs. Therefore, monocrystals may be formed while reduction processes progress at a slow pace. Adsorption of PVP and

nternal/external flaws in NPs significantly affect their form. The authors in [42] found that out of all the nuclei that were created using the citrate approach, one had crystalline, penta-twinned, planar-twinned, and complicated multiply-twinned structures. On the edges of neighboring nanotubes, defects such as steps, kinks, and stacking-faults were discovered. To put it another way, they are reactive places where nanomaterials can develop. The combinations of water, methanol, HAuCl₄, and PVP produced the highest yield of flat hexagonal Au NPRs via plasmon-driven synthesis. These mixtures also included the most planar-twinned seeds. The notion put out by Lofton, Sigmund, who suggested a mechanism for the formation of enormous planar prisms, is confirmed by this research. On the basis of [43], the same NPs are guided to form high-aspect-ratio prisms or plates by the (111) planes of the Au and Ag nuclei. This happens when adatoms attach to the newly formed hollow grooves, which reduce the nucleation energy and cause the prism to develop laterally by forming a new atomic layer in that area. Figure 3 shows the results of a scanning electron microscopy (SEM) investigation of the NPR's side faces, which may have highlighted the function of the Lofton-Sigmund process in the NPR's flattening. The rounded features of these faces should provide for striking contrast when photographing various areas of them. This experiment does not provide any NPR that exhibits such a disparity. The majority of NP display a side picture that is equivalent to 220 gold faces. You can see an example of this kind of NPR in Figure 3a,b.

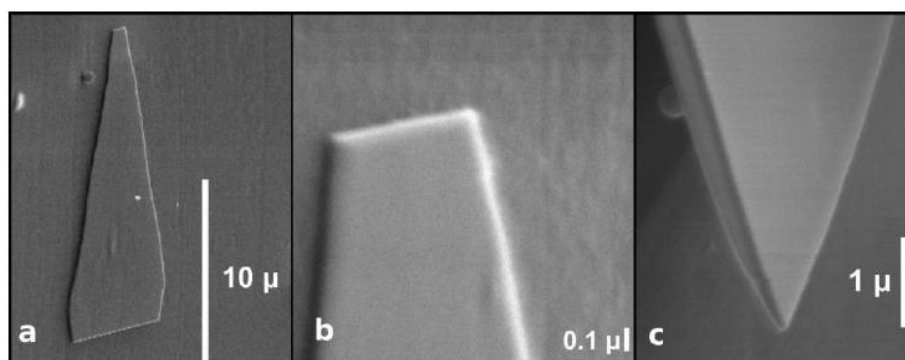


Figure 3: SEM image of hexagonal NPR (a) and part of it (b), (c) concave shape of NPR obtained at tilt of substrate to electron beam of 79°

The picture that may be used to prove the concave shape of the side face is only obtained for very uncommon NPRs that are grown on glass substrates. Figure 3c shows an example of the picture. The top and bottom portions of the side face are noticeably different in brightness. This discrepancy is consistent with the concave shape of the face and could be caused by the varied angles at which different portions of the face are angled toward the electron beam. Based on these results, we hypothesized that the variation in PVP adsorption across the gold faces was the primary factor in the development of flat NPR in our studies. Nevertheless, more research is required to definitively determine the process of NPRs creation. The truncated octahedron is the equilibrium form of Au NPs [44]. The obtained microprisms, which have a surface energy of many tens of nanometers, deviate significantly from this form. This symmetry must be violated in order to produce particles with plate forms. We primarily focus on two symmetry breaking mechanisms. Nanocrystals were hypothesized to have twin flaws or stacking faults in the works cited in [42] and [45]. Adatoms love to adhere to the twin plates' reentrant grooves because of their concave form. Capping agents, primarily surfactants, were thought to have a significant role in the creation of gold nanoplates according to another method. When gold nanostructures are being formed, what part does PVP play? To begin, PVP molecules lower the surface energy of the substrate and alter its surface conditions by adsorbing on substrate imperfections (see to Table 1, line 4 for more information on this). Fixation of AuCl₄-ions on the substrate and subsequent nucleus formation are determined by PVP adsorption on the substrate. Prior to reduction, PVP molecules may form a complex with AuCl₄⁻, allowing them to coordinate with one another [46]. Subsequently, in contrast to the system devoid of PVP, Au (3+) ions undergo reduction under more "soft" circumstances, resulting in the formation of Au clusters with a smaller diameter and a narrow size distribution. The pyrrolidone ring plays a crucial function in the synthesis of Au NPRs [42]. Micro-Raman spectroscopy validated the link between PVP and the Au surface as being formed by an unshared electron pair of oxygen and nitrogen (the pyrrolidone ring) [38]. Secondly, the development of Au NPRs in the (111) direction is inhibited because PVP molecules are adsorbed on their (111) sides, according to a number of studies [47–49]. Consequently, NPRs expand laterally and have a thickness in the tens of nanometer range. To pinpoint where PVP molecules were located on Au NPRs, the Nano SIMS technique was used in [42]. Results showed that PVP is mostly adsorbed on NPRs' peripheries. The preference for PVP adsorption on the (111) faces persisted even when the concentration was increased. Under these circumstances, NPRs synthesized exhibited a doubling of their thickness. In contrast to [42], we use PVP concentrations that are an order of magnitude greater. Therefore, we assume that PVP adsorption is more intense on the flat faces (111), both sides of NPR. The deposited PVP layer prevents gold atoms from diffusing to the NPR surfaces, leading to lateral growth preferentiality. Consequently, we saw NPRs that were flat (10–20 nm thickness) and had lateral sizes of up to 10 microns. Lastly, the particles are protected from aggregating by the PVP molecules that have been adsorbed on them.

The presence of a PVP-stabilizer causes flat NPRs to develop in a layered and tangential fashion, according to the Stranski-Krivanec theory of crystal formation. Stepped terraces are formed by unfinished layers of (111) of NPRs surface, as seen in [38]. Figure 4c and d make it easy to see the development stages of the nanoprisms that match the faces (110) and (100). The atoms of gold are being contained the unfinished layer is formed by breaking the stages. By being preferentially adsorbed on Au (111), PVP molecules block the surface atom delivery and therefore the creation of a new crystal layer. Typically, Au NPRs grow laterally, resulting in crystals that are both thin and flat (Figure 4a and b). Therefore, NPRs may be used as atomically flat substrates for STM after being cleaned from the stabilizer layer, and they have a maximum surface area of 111 [20,50].

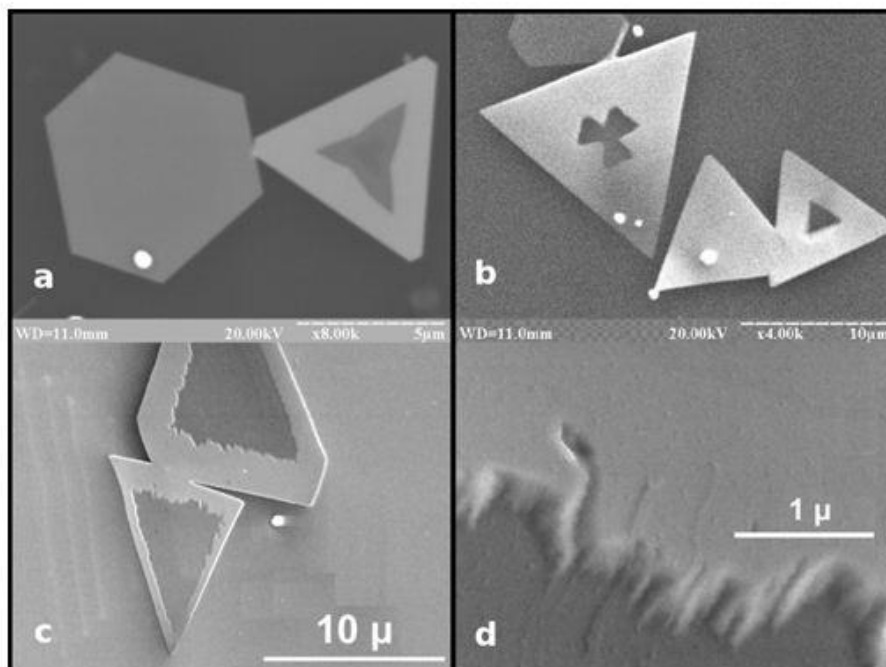


Figure 4: SEM images of the "pits" in nanoprisms

The steps of mica substrate are clearly seen through the two NPRs (Figure 5a). It confirms that the thickness of nanoprisms is in the nanometer range. Extraordinary position of two NPRs is shown in Figure 5b. The lower NPRs has the three petals shape, the upper-a triangle with truncated vertices. It is known that the growth of new atomic layer of the crystal begins at the vertices and edges where the supersaturation of atoms is maximal. Therefore, the formation of dihedral/triangular angle is energetically more favorable. Due to difference in diffusion caused by mutual arrangement of NPRs, the edges of a lower prism growth from vertices to centers. There are also cases when the mutual position of the edges of nanoprisms is parallel (Figure 5c). Slit between them is ~ 300nm.

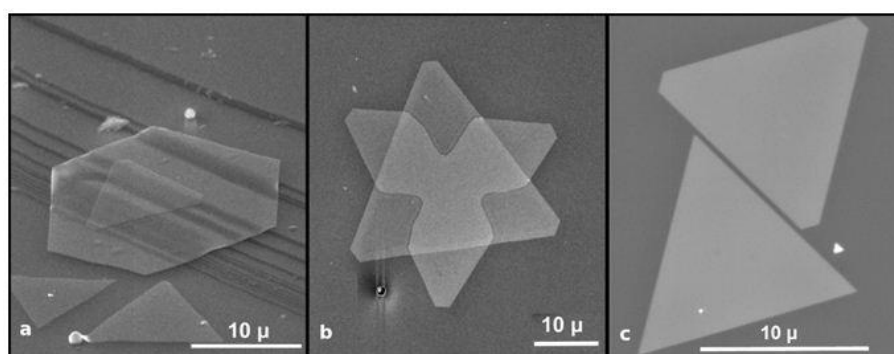


Figure 5: The mutual arrangement of gold nanoprisms on mica surface

Conclusion

Flat Au nanoprisms on mica surfaces may be produced by varying the synthesis conditions. The results demonstrate that the growth medium's viscosity is enhanced by the addition of glycerol. The value of Θ ET:EG is twice as big as \dot{R} ET:EG:G, according to a set of studies conducted on the surface wetting angle Θ . Therefore, a greater wettability is assumed by a lower θ value. In contrast to the ET:EG (1:3) system, introducing PVP to a dispersion medium of ET: EG: G (6:7:7) does not render the surface of mica lyophobic. Gold atoms diffuse less slowly from the bulk to the surface of the crystal and less laterally along the surface of the developing edge due to preferential adsorption of PVP molecules on the faces (111) and an increase in the viscosity of the growth media. It results in the creation of flat surfaces and holes in NPRs. The growing medium G:EG:ET (7:7:6), which contains 0,045M PVP and 1mM HAuCl₄, is more efficient for synthesizing Au NPRs on mica substrate. When these parameters are satisfied, the density of nanoprisms relative to surface area increases.

References

1. Gold nanoparticles: From nanomedicine to nanosensing (Chen PC, Mwakwari SC, Oyelere AK, 2008). Applied Nanotechnology 1: 45–66. El-Sayed IH, El-Sayed MA, Huang X, Jain PK (2008) Nanoscale noble metals: photothermal and optical characteristics, with potential uses in sensing, imaging, biology, and medicine. The article is published in Acc Chem Res and has the DOI: 1077788. Thirdly, in 2015, Pekamwar SS, Deshmukh VS, and alyankar TV Biomedical uses of gold nanoparticles. International Research Journal of Pharmaceuticals, 6: 693-702.
4. A study conducted by Baptista et al. (2008) used gold nanoparticles in the creation of diagnostic tools for therapeutic use. Publication: Anal Bioanal Chem 391: 943-50.5. Jinghong Li, Zhouping Wang, and Jianqiang Hu (2007) Managed Synthesis of Gold Nanoparticles with Enhanced Surface Raman Scattering and Their Use in Biodetection. Article cited as Sensors (Basel)7: 3299-3311. 6. Huang X, Jain PK, El-Sayed IH, El-Sayed MA (2008) Investigating the Use of Gold Nanoparticles in Plasmonic Photothermal Therapy (PPTT). Medical Science Lasers 23: 217–228.
7. A biocomposite of chitosan, glucose oxidase, and gold nanoparticles produced by one-step electrodeposition: a glucose biosensor (Luo XL, Xu JJ, Du Y, Chen HY, 2004). The published version of this article is Anal Biochem 334: 284–96. In 2008, Stewart et al. published a paper titled "Nanostructured Plasmonic Sensors" in the Chemical Reviews, volume 108, pages 494-521. The paper "Electrically-driven optical antennas" was written by Kern et al. (2015). Scientific Reports, Volume 9, Issue 6, Page 582-6. 10. A Group of Researchers Led by Christian Huck, Andrea Toma, Frank Neubrech, Manohar Chirumamilla, Jochen Vogt, and Others (2015) Enhanced Plasmonic Performance in the Infrared using Gold Nanoantennas on a Pedestal ACS Photon 2: 497-505. Atomically flat single-crystalline gold nanostructures for plasmonic nanocircuitry, published in 2010 by Huang JS, Callegari V, Geisler P, Brüning C, Kern J, and others. Public Health 1: 350–7.12. The Memory Effect of a Polymer Thin-Film Transistor with Self-Assembled Gold Nanoparticles in the Gate Dielectric was studied by Zhengchun Liu, Fengliang Xue, Yi Su, Yuri M. Lvov, and Kody Varahramyan in 2006. IEEE Transactions on Nanotechnology, 5(3), 379–384. 13. Pooi See Lee, Srinivasan MP, Gao Ying, and Raju Kumar Gupta (2012) Covalent Bonding of Gold Nanoparticles: A Prospective Use in Memory Transistors. J Published in Physical Chemistry B 116: 9784-90. Xu, Kong, and Chen (2009) used single-molecule techniques to investigate the heterogeneity and catalytic activity of gold nanoparticles. The citation is from the journal Physical Chemistry Chemical Physics, volume 11, pages 2767–47. 15. Gold as a New Catalyst in the Modern Era: Synthesis, Mechanism of Action, and Potential Uses (Haruta M., 2004). Journal of Gold Mining and Metallurgy, 37, 27, 1936. Masatake and Masakazu (2001) made significant progress in the field of gold nanoparticle catalysis. Current Catalysis 222: 427–437.
2. Review of substrate manufacturing for surface enhanced Raman spectroscopy and its analytical chemistry applications (17. Fana M, Andrade GF, Brolo AG, 2011). Journal of Anal Chem 693: 7-25. 18. Gold nanocrystals as a substrate for micro Raman spectroscopy (Borodinova TI, Kravets VG, Romanyuk VR 2012). Johns Hopkins University Journal of Nano-Electron Physics 4(1): 1-8. 19. "Gold Nanoparticle Superlattices: Novel Surface Enhanced Raman Scattering Active Substrates" (2009, Shibu ES, Kimura K, Pradeep T). In their 2006 work published in Chem Mater, Dahanayaka DH, Wang JX, Hossain S, and Bumm LA discuss the use of flat gold nanoparticle platforms for high-resolution scanning tunneling microscopy, as well as optically transparent Au{111} substrates. Journal of the American Chemical Society 128: 6052-3. 21. Sajanlal PR, Pradeep T (2008) Growth of anisotropic gold nanostructures on conducting glass surfaces. J The article "Movable Au Microplates as Fluorescence Enhancing Substrates for Live Cells" was published in the journal Chemical Science in 2010 and can be found on page 79–85. Sau TK, Murphy CJ (2004) Room Temperature, High-Yield Synthesis of Multiple Shapes of Gold

Nanoparticles in Aqueous Solution. *Nano Research* 3: 738–747. Published in the Journal of the American Chemical Society, volume 126, pages 8648–8649, this work by Millstone et al. (2005) describes the discovery of a quadrupole plasmon mode in a colloidal solution of gold nanoprisms. Millstone JE, Métraux GS, and Mirkin CA (2006) Controlling the edge length of gold nanoprisms using a seed-mediated method was published in the Journal of the American Chemical Society, volume 127, pages 5312-3. The controlled assembly of gold nanoprism and hexagonal nanoplate films for surface enhanced Raman scattering was published in *Adv Func Mater*, volume 16, pages 1209–14, in 2011. The authors are Lee, Hong, and Park. Scarabelli et al. (2014) published a study in the Journal of the Korean Chemical Society on monodisperse gold nanotriangles, discussing their size control, large-scale self-assembly, and performance in surface-enhanced Raman scattering. The study was published in volume 32, pages 3575–3580. *ACS Nano*, volume 8, pages 5833–5842, 2010. 28. Estela-Llopis VR, Borodinova TI, Yurkova IN. Gold and platinum nano- and microcrystals synthesized in poly-saccharide water solutions by extracellular biomineralization. This is in the book "Nano-Science: Colloidal and Interfacial Aspects." Vol. 3, Issue 2, Pages 307–368, Edited by V.M. Starov, CPC Press Taylor&Francis Group, LLC, London, New York. Nanoparticles and nanoplates made of gold using a cell extract from *Shewanella* algae were synthesized at room temperature in 2010 by Ogi, Saitoh, Nomura, and Konishi. The biological production of triangular gold nanoprisms was described by Shankar SS, Rai A, Ankamwar B, Singh A, Ahmad A, et.al. (2004) in the Journal of Nanopart Research, volume 12, pages 2531–2539. Nourishing Matter 3: 482–482. Endophytic *Aspergillus clavatus* Extract for Biofabrication of Anisotropic Gold Nanotriangles: A Dual-Functional Reductant and Stabilizer (Verma VC, Singh SK, Solanki R, Prakash S., 2011). *Research Letters, Nanoscale* 6:16. In 2010, Miranda et al. (32 researchers) analyzed the data from Malheiro, Skiba, Quaresma, and Carvalho. An efficient method for producing triangular gold nanoplates with a wide range of adjustable edge lengths in a single reaction. *Microscale* 2: 2209–216. Number thirty-three, Chu, Kuo, and Huang (2006) Method for the Thermal Aqueous Solution Synthesis of Three-Dimensional Hexagonal and Triangular Gold Nanoplates. *Organic Chemistry* 45: 808-813. The authors of the 2004 study are Kim, Connor, Song, Kuykendall, and Yang. Nanocrystals of platonic gold. *Angewandte Chemie International Edition*, 43, 3673–3677, 2017. Mass Synthesis of Large, Single-Crystal Au Nanosheets Based on a Polyol Process (Li BC, Cai W, Cao B, Sun F, Li Y, et.al., 2006). *Journal of Advanced Functional Materials*, 16(1), 83–90. Using binary surfactants as a rapid growth aid, Wang et al. (2010) synthesized high-yield gold nanoplates. *Journal of Nanomaterials*, 2010: 9. 37. Liuab and Yang (2011) A two-step method for heating gold nanoplates that improves their optical and surface Raman spectra. 38. Borodinova TI, Sapsay VI, Romanyuk VR (2015) published in *CrystEng- Comm* 13: 2281-8. A Solution for the Formation of Gold Nanocrystals Containing Primary Alcohols. A study conducted by Wang et al. (2010) titled "Synthesis of High-Yield Gold Nanoplates: Fast Growth Assistant with Binary Surfactants" was published in the Journal of Nano-Electron Physics, volume 7, issue 10, and was referenced as reference 39. *Journal of Nanomaterials* 2010: 9. 40. Tsuji et al. (2007) used oxidative etching by AuCl₄⁻ and Cl⁻ anions in a microwave-polyol method to regulate the shape and size of gold nanocrystals. Cohesion and Exposed Surfaces The theory, production, and mechanism of formation of monodispersed hydrosols was published by LaMer VK and Dinegar RH in 1950 in the journal *Physicochemical Engineering Part A*, Volume 302:588–589. In plasmon-driven synthesis, polyvinylpyrrolidone induces anisotropic development of gold nanoprisms; 42. Zhai Y, DuChene JS, Wang Y-Ch, Qiu J, Johnston-Peck AC, et.al. (2016). Chapter 43 of *Nature Materials*, published in 2005 by Lofton and Sigmund, discusses the processes that govern the crystal structures of colloidal gold and silver. *Scientific Reports*, Volume 15, Issue 10, Pages 1197–208. 44. Equilibrium Morphology of Face-Centered Cubic Gold Nanoparticles >3 nm and the Shape Changes Induced by Temperature, Published by Barnard AS, Lin XM, and Curtiss LA in 2005. *Physical Journal Chemistry Letters* 109, 24465-72, 2009 by Younan Xia, Yujie Xiong, Byungkwon L., and Sara ES. 45. Shape-Controlled Synthesis of Metal Nanocrystals: When Simple Chemistry Meets Complex Physics? The subject of *Journal of Chemical Education and Research*, 48, 60–103. 46. Yonezawa T, Toshima N (1995). A Mechanistic Analysis of the Production of Nanoscale Bimetallic Clusters Protected by Polymers. In 2004, Tsuji et al. published a paper titled "Microwave-assisted Synthesis of Metallic Nanostructures in Solutions" in the Journal of the Chemical Society's *Faraday Transactions*, volume 91, pages 4111–4119. Using Aging to Control the Size of Ultrasonically Induced Au Nanoprisms and Related Topics, *Chem. Eure. J.* 11: 440–52 (2006). 48. Li C, Cai W, Li Y, Hu J, Liu P. James P. *Chem. B.* 110: 1546–152. 49. Triangular nanoprisms made of colloidal gold and silver, published in 2009 by Millstone JE, Hurst SJ, Métraux GS, Cutler JI, and Mirkin CA. Volume 5, pages 641-646, 50. Preparing supported flat gold nanoparticles for use as Au (111) single crystal substrates was the topic of Dahanayaka DH and Bumm LA's 2010 presentation at the AVS 57th International Symposium & Exhibition on Nanoscale Science and Technology.